

THERMAL DECOMPOSITION KINETICS OF LANTHANUM OXALATE HYDRATE PRODUCT TREATMENT FROM MONAZITE

M.V. Purwani¹, Suyanti¹ and Wisnu Ari Adi²

¹Center for Accelerator Science and Technology, BATAN
Jl Babarsari 21, Yogyakarta, Indonesia

²Center for Science and Technology of Advanced Materials, BATAN
Gedung 42, Kawasan Puspiptek Serpong

E-mail: purwanimv@gmail.com

Received: 3 October 2018

Revised: 11 December 2018

Accepted: 19 December 2018

ABSTRACT

THERMAL DECOMPOSITION KINETICS OF LANTHANUM OXALATE HYDRATE PRODUCT TREATMENT FROM MONAZITE. Unreacted shrinking core model variation was developed for calcination and solid thermal decomposition reaction to non-catalytic gas and no gas reactants were involved. In this research, thermal decomposition of lanthanum oxalate hydrate product treatment of monazite was studied. The parameters for modeling are time and temperature of thermal decomposition. The time was between 0 - 150 minutes with 30 minutes intervals and the temperature range between 600 - 700 °C with 100 °C intervals. Based on the experimental data it can be concluded that the most suitable model was unreacted core sphere ash diffusion controls and obtained the relation between temperature T °C with diffusion coefficient D following equation $D = 0.0011 T + 0.5175$ with linearity $R^2 = 0.9561$. Another possible model was the sphere reaction control and obtained the relationship between $1/T$ (K) and reaction rate constant k_s was $k_s = 48873.e^{-4.88 / RT}$ with activation energy = 4.88 kJ. The relationship between time t with r_c (radius of particles at time t) at various temperatures and the relation between temperature and r_c at various times follows the exponential line equation. If temperature and time parameters were combined, the relation between time and temperature with r_c following the equation $\ln r_c = -0.9536 (9E-04T + 0.005t) + 4.9976$ will be found.

Keywords: kinetics, thermal decomposition, lanthanum oxalate hydrate

ABSTRACT

DEKOMPOSISI TERMAL KINETIK PADA LANTHANUM OXALATE HYDRATE HASIL PERLAKUAN DARI MONAZITE. Variasi model inti dari penyusutan yang tidak bereaksi telah dikembangkan untuk kalsinasi dan reaksi posisi dekomposisi termal pada gas non katalitik dan tidak ada reaktan gas yang terlibat. Dalam penelitian ini, dekomposisi termal perlakuan produk hidrat lantanum oksalat monazit telah dilakukan. Parameter untuk pemodelan adalah waktu dan suhu dekomposisi termal. Waktu antara 0 - 150 menit dengan interval 30 menit dan kisaran suhu antara 600 - 700 °C dengan interval 100 °C. Berdasarkan data eksperimen dapat disimpulkan bahwa model yang paling cocok adalah kontrol difusi inti bola yang tidak bereaksi dan diperoleh hubungan antara suhu T °C dengan koefisien difusi D berikut persamaan $D = 0,0011T + 0,5175$ dengan linearitas $R^2 = 0,9561$. Model lain yang memungkinkan untuk dilakukan adalah kontrol reaksi bola dan memperoleh hubungan antara $1/T$ (K) dan konstanta laju reaksi k_s adalah $k_s = 48873e^{-4,88/RT}$ dengan energi aktivasi = 4,88 kJ. Hubungan antara waktu t dengan r_c (jari-jari partikel pada waktu t) pada berbagai suhu dan hubungan antara suhu dan r_c pada berbagai waktu mengikuti persamaan garis eksponensial. Jika parameter suhu dan waktu digabungkan akan menemukan hubungan antara waktu dan suhu dengan r_c mengikuti persamaan $\ln r_c = -0,9536 (9E-04 T + 0,005 t) + 4,9976$.

Kata kunci: kinetik, dekomposisi termal, lanthanum oxalate hydrate

INTRODUCTION

Sustainable technological development is strongly dependent on new materials with particular mechanical, chemical, electrical, magnetic, or optical properties. In order to address this challenge, interdisciplinary research technologies, to develop new materials, especially inorganic materials, to impart new

functional properties and to provide new processing methods for the formation of useful objects are under intense focus [1,2]. Within the class of inorganic materials, oxides perform various functions [3]. The oxide ceramics are well known materials for technical applications, particularly in electronic and structural areas.

The purity of these materials is extremely important. In the oxide class, lanthanum oxide (La₂O₃) is one of the most widely studied over the years. Lanthanum oxide has been widely applied to many industrial applications. For example, it is an important component of automobile exhaust-gas conversion [4], as a catalyst support in the formation of gas conversion catalyst [5] and as a catalyst of oxidative coupling of methane [6]. It is also used as a refractory oxide for calcium lights, optical glass [7] and in the formation of ceramics as a core for carbon arc electrodes and lanthanum oxide is also used as a raw material for radar absorption (RAM) [8]. However, as the raw material in these fields, synthesis of lanthanum oxide with good quality is very important [9].

The rare earth oxide can be prepared by oxalate thermal decomposition, but its characteristics on a great degree depend upon the calcining conditions. Thus, monitoring the process of oxalate thermal decomposition is an important issue [9]. Balboul et al [5] had reported that the characteristic of thermal decomposition of lanthanum oxalate decahydrate La₂(C₂O₄)•10H₂O to the onset of La₂O₃ could be measured by thermogravimetry (TG) and different thermal analysis (DTA). The characteristics of the lanthanum oxalate decahydrate and the activation energy of the observed thermal processes were obtained by means of IR-spectroscopy, X-ray diffractometer, but kinetic of thermal analysis of various compounds is of major importance because of their frequent applications in calcination metallurgy and in the production of sorbents and catalysts with large-surface materials [10]. Unfortunately, most literatures rested on the understanding of the activation energy of the thermal processes and few people paid attention to the kinetics and the most probable model of thermal decomposition. Compared with other methods, thermal decomposition process has many advantages, such as more effective control of size and shape of the particle, shorter preparation time and fewer impurities in the final product [11,12]. Thermal decomposition methods were preferably used to prepare the nanostructure ceramic materials [13,14]. In the future, the exploitation of such lanthanide oxide architectures by thermal decomposition may provide an opportunity of producing innovative ceramic materials with novel and tunable magnetic, electronic, or

catalytic properties [15]. At present, the ultra-fine La₂O₃ powder can be prepared by solid phase, hydrothermal synthesis, precipitation, sol-gel and micro-emulsion methods. Among these methods, precipitation method is used widely for its simplicity. High and uniform super-saturation is the key factor to affect the size of the “ultra fine” solid particles in precipitation. In order to obtain the high and uniform super-saturation, a kind of new reactor, submerged circulative impinging stream reactor (SCISR), was developed [16].

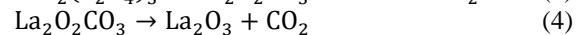
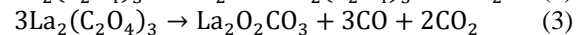
In this work, La₂(C₂O₄)₃•10H₂O was prepared from monazite sand. The thermal decomposition of La₂(C₂O₄)₃•10H₂O was conducted from 600 °C to 1000 °C in furnace. The intermediate product and the final solid product are analyzed by X-ray fluorescence (XRF) and X-ray diffractometer (XRD).

Kinetic decomposition was studied by applying unreacted shrinking core model [17]. The influence of different temperature regions upon the thermal behavior of chemical compounds can provide kinetic parameters indicating change in the reaction pathway. The complexity of a stage can be expressed from the activation energy (*E*) dependent on the extent of conversion (*α*). The activation energy can be obtained by isoconversional method. If *E* does not depend on *α*, the investigated process is a simple one and should be described by a unique kinetic triplet. Otherwise, the process will be complex. In this work integral isoconversional methods were used to analyze the non-isothermal kinetics of the lanthanum oxalate. The extent of conversion, *α*, is defined by the following equation [18]:

$$\alpha = (m_0 - m)/(m_0 - m_f) \quad (1)$$

Where *m* is the mass of the sample at a given time *t*; *m*₀ and *m*_{*f*} refer to masses at the beginning and the end.

The stages of reaction that occurred [19,20]:



The description and development of solid particle reaction including intermediate formation has been studied before [21]. The mechanism and mathematical models of thermal decomposition also been studied with the summary as attached in Table 1 [22].

Table 1. The mechanisms occurring and mathematical models of thermal decomposition [22]

Mechanisms		Mathematical models
Constant size particle		
Sphere	Sphere Film Diffusion Controls	$\alpha = \frac{3bk_s}{\rho_B R} t$ (5)
	Sphere Ash Diffusion Controls	$1 - 3(1 - \alpha)^{\frac{2}{3}} - 2(1 - \alpha) = \frac{6bD}{\rho_B R^2} t$ (6)
	Sphere Reaction Controls	$1 - (1 - \alpha)^{1/3} = \frac{bk_s}{\rho_B R} t$ (7)
Cylinder	Cylinder Film Diffusion Controls	$\alpha = \frac{2bk_s}{\rho_B R} t$ (8)
	Cylinder Ash Diffusion Controls	$\alpha + (1 - \alpha) \ln(1 - \alpha) = \frac{4bD}{\rho_B R^2} t$ (9)
	Cylinder Reaction Controls	$1 - (1 - \alpha)^{1/2} = \frac{bk_s}{\rho_B R} t$ (10)
Shrinking sphere		
Small particle	Small Particle Film Diffusion Controls	$1 - (1 - \alpha)^{2/3} = \frac{2b \cdot D}{\rho \cdot y \cdot r_0^2} t$ (11)

Mechanisms		Mathematical models
Constant size particle		
Stokes Regime	Small Particle Ash Diffusion Controls	Not applicable
	Small Particle Reaction Controls	$1 - (1-\alpha)^{1/3} = \frac{bks}{\rho_B R_0} t$ (12)

where:

- k = surface reaction rate constant ($\text{mol}^{-n} \text{m}^3 \text{n}^{+1}/\text{s}$)
- b = stoichiometric factor
- ρ_B = particle density, g/mL
- t = heating time, minutes,
- D = diffusion constant, g/cm^2 or mole/cm^2
- R_0 = the radius of the initial particle (initial radius) at time = 0

If the mechanism was controlled by the rate of reaction, the relationship between the rate coefficient and $1/T$ obeys the Arrhenius equation [23]:

$$k = k_0 e^{-E/RT} \quad (13)$$

- k = surface reaction rate constant ($\text{mol}^{-n} \text{m}^3 \text{n}^{+1}/\text{s}$)
- k_0 = Arrhenius pre-exponential coefficient
- E = activation energy, kJ
- A = frequency factor

The composition analysis or element content (%) using XRF were presented in Table 2. Apparently La oxalate still contains cerium oxalate.

Table 2. The content or composition of the oxalate compound

Compound	Content (%)
$\text{La}_2(\text{C}_2\text{O}_4)_3 \cdot 10 \text{H}_2\text{O}$	92.87
$\text{Ce}_2(\text{C}_2\text{O}_4)_3$	2.91
Water	4.22

EXPERIMENTAL METHOD

Materials

The material used was Lanthanum oxalate product treatment of monasite sand.

Equipment

Glassware, scales, oven, high temperature furnace 1500 °C, X-ray fluorescence (XRF) were used as the equipment.

Methods

Solids of $\text{La}_2\text{C}_2\text{O}_3 \cdot 10\text{H}_2\text{O}$ was weighed as much as 5 grams and heated at a temperature of 600 °C in a high temperature furnace for various time, e.g. 30, 60, 120 and 150 minutes. After cooling, obtained solid were reweighed. The procedure was repeated for various temperature, those are 700 °C, 800 °C, 900 °C and 1000 °C. Analysis of lanthanum oxalate composition and thermal decomposition results using XRF.

Effect of decomposition time on weight, fraction and conversion of solid weight at various temperatures

The weight conversion calculation uses the following formula (equation 1). Where α is $(m_0 - m) / (m_0 - m_f)$ which m_0 is the initial mass (5 g) and m_f is the final mass (2.17 g, when it has turned into La oxide).

The effects of increasing time and temperature of heating, there will be a reduction in weight and weight fraction, but the weight conversion of α is greater [24,25]. At first heating the free water will evaporate, then the crystal water decomposes (stage I). If the heating continues and the temperature was higher, there will be decomposition phase II that was formed La oxycarbonate and finally decomposition phase III was occur that was formed La oxide. The relationship between heating time with weight, weight fraction and weight conversion α at various temperatures were presented in Figure 1a, Figure 1b and Figure 1c.

RESULTS AND DISCUSSIONS

Analysis of Lanthanum Oxalate Composition

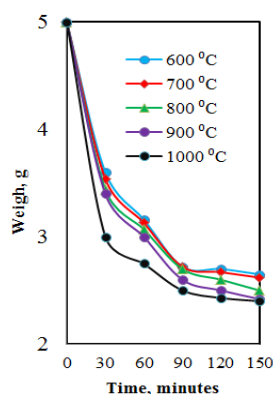


Figure 1a. The relationship between heating time and weight after heating at various temperatures

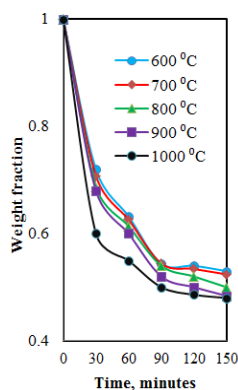


Figure 1b. The relationship between heating time and weight fraction after heating at various temperatures

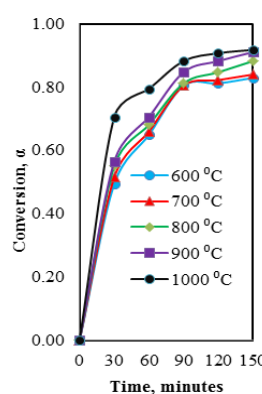


Figure 1c. The relationship between heating time and conversion after heating at various temperatures

Table 3. The equation of the relationship between t and f(α) at various temperatures for sphere film diffusion controls, sphere ash diffusion controls, sphere reaction controls

Temperatures, °C	Sphere Film Diffusion Controls	Sphere Ash Diffusion Controls	Sphere Reaction Controls
600	$y_{600} = 0.005x + 0.2231$	$y_{600} = 0.003x + 0.0287$	$y_{600} = 0.0029x + 0.0825$
700	$y_{700} = 0.005x + 0.2311$	$y_{700} = 0.0031x + 0.031$	$y_{700} = 0.0029x + 0.0857$
800	$y_{800} = 0.0052x + 0.2411$	$y_{800} = 0.0035x + 0.0272$	$y_{800} = 0.0032x + 0.086$
900	$y_{900} = 0.0054x + 0.2486$	$y_{900} = 0.0039x + 0.095$	$y_{900} = 0.0034x + 0.1401$
1000	$y_{1000} = 0.0054x + 0.3243$	$y_{1000} = 0.004x + 0.0262$	$y_{1000} = 0.0035x + 0.0867$
Notes	$y = f(\alpha) = \alpha$ $x = t = \text{temperatures}$	$y = f(\alpha) = 1 - 3(1 - \alpha)^{\frac{2}{3}} - 2(1 - \alpha)$ $x = t = \text{temperatures}$	$y = f(\alpha) = 1 - (1 - \alpha)^{1/3}$ $x = t = \text{temperatures}$

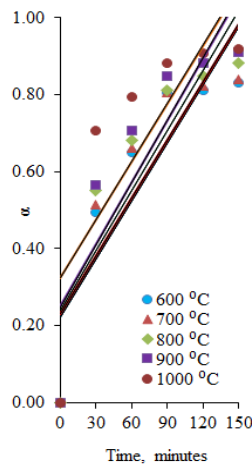


Figure 2a. The relationship time with α, at various temperatures (Cylinder Film diffusion control)

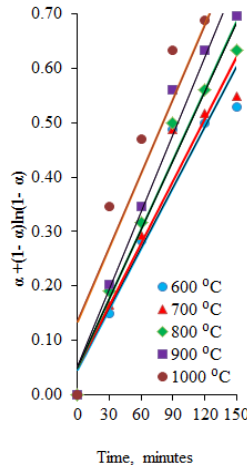


Figure 2b. The relationship time with $\alpha + (1 - \alpha) \ln(1 - \alpha)$, at various temperatures (Cylinder Ash diffusion control)

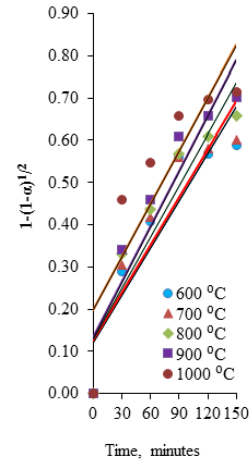


Figure 2c. The relationship time with $1 - (1 - \alpha)^{1/2}$, at various temperatures (Cylinder Reaction control)

Determination of Mechanisms and Mathematical Model

The calculation of conversion values can be arranged model of shrinking particle both the constant size particle with the sphere and the cylinder shape, as well as shrinking sphere particles. The equation of the relationship between time (t) with f(α) for sphere film diffusion controls, sphere ash diffusion controls, sphere reaction controls shown in Table 3.

The relation between time (t) and the weight conversion equation $\alpha = f(\alpha)$ for the constant size particle of the spherical shape were shown in Figure 2a, Figure 2b and Figure 2c. The function $\alpha = f(\alpha)$ for each model according to equations (5), (6) and (7). Preparation of the relationship between t with f(α), was very important in order to select the model of mathematical equations that describe events that occur and that control.

The equation of the relationship between time (t) and f(α) for cylinder film diffusion controls, cylinder ash diffusion controls and cylinder reaction controls are shown in Table 4a.

While, the equations line linearity (R²) of the relationship between time (t) and f(α) for the cylinder film diffusion controls, cylinder ash diffusion controls and cylinder reaction controls were shown in Table 4b. The relationships between time and the weight conversion equation $\alpha = f(\alpha)$ for the Shrinking Sphere particle are shown in Figure 4a and Figure 4b. The function $\alpha = f(\alpha)$ for each model is according to equations (11) and (12).

The equations of the relationship between time (t) and f(α) for small particle film diffusion controls and small particle reaction controls were shown in Table 5a.

Table 4a. The equation of the relationship between t and f(α) at various temperatures for cylinder film diffusion controls, cylinder ash diffusion controls and cylinder reaction controls

Temperature, °C	Cylinder Film Diffusion Controls	Cylinder Ash Diffusion Controls	Cylinder Reaction Controls
600	$y_{600} = 0.005x + 0.2231$	$y_{600} = 0.0037x + 0.0462$	$y_{600} = 0.0037x + 0.1216$
700	$y_{700} = 0.005x + 0.2311$	$y_{700} = 0.0038x + 0.05$	$y_{700} = 0.0038x + 0.1264$
800	$y_{800} = 0.0052x + 0.2411$	$y_{800} = 0.0042x + 0.0489$	$y_{800} = 0.0041x + 0.1291$
900	$y_{900} = 0.0054x + 0.2486$	$y_{900} = 0.0047x + 0.0506$	$y_{900} = 0.0044x + 0.1318$
1000	$y_{1000} = 0.0054x + 0.3243$	$y_{1000} = 0.0045x + 0.1354$	$y_{1000} = 0.0042x + 0.1983$
Notes	$y = f(\alpha) = \alpha$ $x = t = \text{temperature}$	$y = f(\alpha) = \alpha + (1 - \alpha) \ln(1 - \alpha)$ $x = t = \text{temperature}$	$y = f(\alpha) = 1 - (1 - \alpha)^{1/2}$ $x = t = \text{temperature}$

Table 4b. The equations line linearity (R²) the relationship between $f(\alpha)$ and t at various temperatures for cylinder film diffusion controls. Cylinder ash diffusion controls and cylinder reaction controls

Temperature °C	Cylinder Film Diffusion Controls	Cylinder Ash Diffusion Controls	Cylinder Reaction Controls
600	R ² = 0.7691	R ² = 0.9184	R ² = 0.8433
700	R ² = 0.7626	R ² = 0.9303	R ² = 0.8451
800	R ² = 0.7668	R ² = 0.9651	R ² = 0.8705
900	R ² = 0.7674	R ² = 0.9614	R ² = 0.879
1000	R ² = 0.6399	R ² = 0.8751	R ² = 0.762

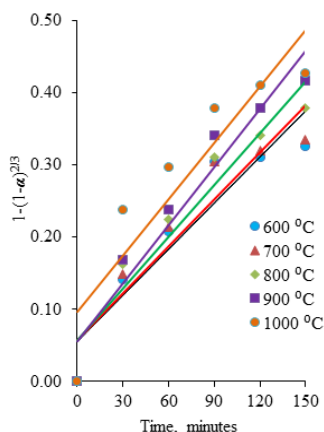


Figure 4a. The relationship between time with $1 - (1 - \alpha)^{2/3}$ at various temperatures (small particle film diffusion controls)

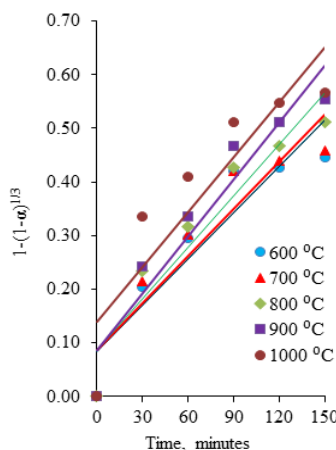


Figure 4b. The relationship between time with $1 - (1 - \alpha)^{1/3}$ at various temperatures (small particle reaction control)

Table 5a. The equation of the relationship between t and $f(\alpha)$ at various temperatures for small particle film diffusion controls and small particle reaction controls.

Temperature °C	Small particle film diffusion control	Small particle Reaction control
600	$y_{600} = 0.0021x + 0.0554$	$y_{600} = 0.0029x + 0.0825$
700	$y_{700} = 0.0022x + 0.0575$	$y_{700} = 0.0029x + 0.0857$
800	$y_{800} = 0.0024x + 0.0566$	$y_{800} = 0.0032x + 0.086$
900	$y_{900} = 0.0027x + 0.0563$	$y_{900} = 0.0035x + 0.0867$
1000	$y_{1000} = 0.0026x + 0.0967$	$y_{1000} = 0.0034x + 0.1401$
Notes	$y = f(\alpha) = 1 - (1 - \alpha)^{2/3}$	$y = f(\alpha) = 1 - (1 - \alpha)^{1/3}$
	$x = t = \text{temperature}$	$x = t = \text{temperature}$

Table 5b. The equations line linearity (R²) the relationship between $f(\alpha)$ and t at various temperatures for small particle film diffusion controls and small particle reaction controls

Temperature °C	Small particle film diffusion control	Small particle Reaction control
600	R ² = 0.878	R ² = 0.8649
700	R ² = 0.8848	R ² = 0.8697
800	R ² = 0.9208	R ² = 0.9018
900	R ² = 0.9311	R ² = 0.9117
1000	R ² = 0.8341	R ² = 0.8057

The equations line linearity (R²) of the relationship between time (t) with $f(\alpha)$ for the small particle film diffusion controls and small particle reaction controls were shown in Table 5b.

The equations of the relationship between time (t) and $f(\alpha)$ for small particle film diffusion controls and small particle reaction controls were shown in Table 5a.

To determine the value of the diffusivity (D) use the formula $f(\alpha) = \frac{6bD}{\rho_B R^2} t$ for the sphere ash diffusion control equation and to determine the

activation energy use the formula $f(\alpha) = \frac{bk_s}{\rho_B R} t$ for sphere reaction control. The relationship between temperature °C (T) and D is presented in Figure 5a and the relationship between $1/T$ ($T^\circ\text{K}$) and $\ln k_s$ ($k_s =$ constant reaction rate) is shown in Figure 5b.

Sphere Ash Diffusion Controls

$$\text{Slope} = \frac{6bD}{\rho_B R^2} \tag{14}$$

with $R = 0.0074$ cm, $\rho_B = 1.5$ g/cm³, $D =$ molecular diffusion coefficient cm²/sec, and $b =$ Coefficient of $\text{La}_2(\text{C}_2\text{O}_4)_3$ reaction.

Sphere Reaction Controls

$$\text{Slope} = \frac{bk_s}{\rho_B R} t \quad (15)$$

With $R = 0.0074 \text{ cm}$, $\rho_B = 1.5 \text{ g/cm}^3$, $b =$ Coefficient of $\text{La}_2(\text{C}_2\text{O}_4)_3$ reaction, and $k_s =$ reaction rate constant.

The relationship between T and D follows the equation

$$D = 0.0011 T + 0.5175 \quad (16)$$

with $R^2 = 0.9561$. The relationship between $1/T$ and $\ln k_s$ follows the equation,

$$\ln k_s = -586.86/T + 10.797 \quad (17)$$

with $R^2 = 0.9115$, $E/R = 586.86$, $R =$ ideal gas law constant $= 8.314 \text{ J/gmol}$, $E =$ activation energy $= 4879.43 \text{ J} = 4.88 \text{ kJ}$, $\ln A = 10.797$ and $A = 48873$.

The relationship equation between k_s with T becomes

$$k_s = 48873e^{-4.88/RT} \quad (18)$$

The shrinking of particle size on Sphere Ash Diffusion Controls can be calculated by the formula:

$$\alpha = 1 - (r_c/R)^3 \quad (19)$$

With $r_c =$ radius of unreacted core at time t (μm) and $R =$ initial radius of particle $= 74 \mu\text{m}$.

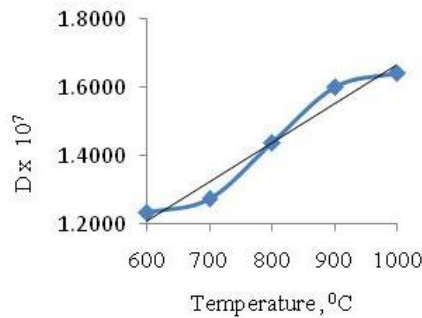


Figure 5a. The relationship between temperature (T) and D

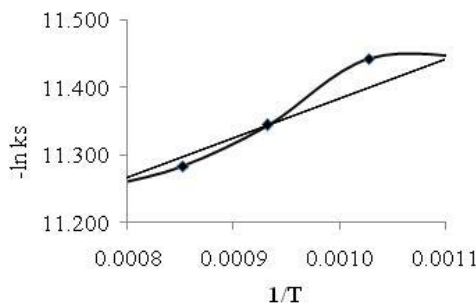


Figure 5b. The relationship between $1/T$ and k_s

The relationship between time t and r_c at various temperatures is shown in Figure 6a and the relationship between temperature $^\circ\text{C}$ and r_c at various times is shown in Figure 6b. The equation of the relationship between time t and r_c at various temperatures is shown in Table 6a and the relationship between temperature $^\circ\text{C}$ and r_c at various times are shown in Table 6b. They follow exponential equations.

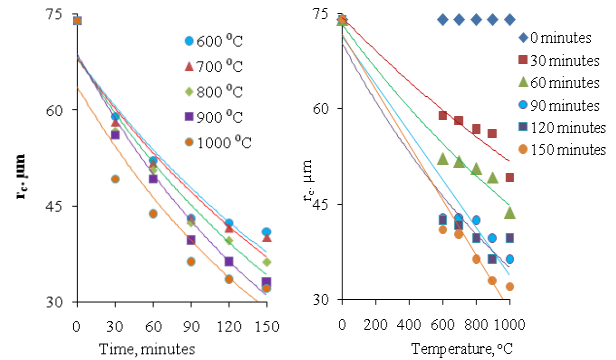


Figure 6a. The relationship between time t and r_c at various temperatures (Sphere Ash Diffusion Controls)

Figure 6b. The relationship between temperature $^\circ\text{C}$ and r_c at various times (Sphere Ash Diffusion Controls)

Table 6a. The equations of relationship between time t and r_c at various temperatures

Temperature, $^\circ\text{C}$	Equation	Linearity (R^2)
600	$y_{600} = 68.12e^{-0.004t}$	$R^2 = 0.9005$
700	$y_{700} = 67.925e^{-0.004t}$	$R^2 = 0.9112$
800	$y_{800} = 68.343e^{-0.005t}$	$R^2 = 0.9529$
900	$y_{900} = 68.663e^{-0.005t}$	$R^2 = 0.9624$
1000	$y_{1000} = 63.532e^{-0.005t}$	$R^2 = 0.8864$

Table 6b. The equations of the relationship between temperature $^\circ\text{C}$ (T) and r_c at various times

Time, minutes	Equation	Linearity (R^2)
30	$y_{30} = 74.334e^{-4E-04T}$	$R^2 = 0.9418$
60	$y_{60} = 73.205e^{-5E-04T}$	$R^2 = 0.9668$
90	$y_{90} = 71.502e^{-7E-04T}$	$R^2 = 0.9595$
120	$y_{120} = 70.212e^{-7E-04T}$	$R^2 = 0.9162$
150	$y_{150} = 72.414e^{-9E-04T}$	$R^2 = 0.9879$

The integration equation of relationship between time with r_c at optimum temperature ($1000 \text{ }^\circ\text{C}$) and equation of relationship between temperature with r_c at optimum time (150 minutes) as follows:

$$r_c = 63.532e^{-0.005t} \cdot 72.414e^{-9E-04T} \quad (20)$$

To make into a linear relationship

$$\ln r_c = -b(0.005t + 9E - 04 T) + a \quad (21)$$

The graph of relationship between $0.005t + 9E - 04 T$ and $\ln r_c$ is shown in Figure 7.

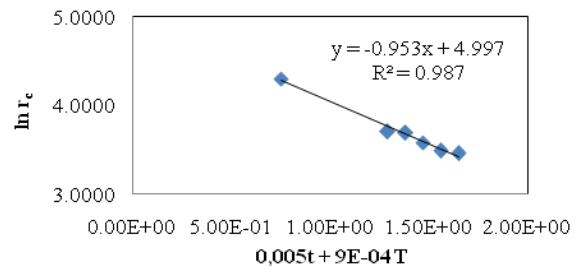


Figure 7. The relationship between $0.005t + 9E - 04 T$ and $\ln r_c$

The relationship between T and t with r_c become:

$$\ln r_c = -0.9536 (9E-04T + 0.005t) + 4.9976 \quad (22)$$

At heating of 1000 °C for 150 minutes, the result of composition of solids based on XRF data after decomposition is shown in Table 7.

Table 7. The Content or Composition of The Lanthanum Compound After Decomposition

Compound	Content (%)
La ₂ O ₂ CO ₃	76.57
La ₂ O ₃	17.70
Ce ₂ (C ₂ O ₄) ₃	5.00
Ce ₂ O ₂ CO ₃	0.73

CONCLUSION

The parameters used for modeling were time and temperature of thermal decomposition. Time range were 0 - 150 minutes with a 30 minutes interval and the temperatures range between 600°C – 700°C with 100°C intervals. From the experimental data, it can be concluded that the most suitable model is unreacted core Sphere Ash Diffusion Controls and obtained the relationship between temperature T °C with diffusion coefficient D follow equation $D = 0.0011T + 0.5175$ with linearity $R^2 = 0.9561$. Another possible model is the sphere reaction control and the relationship between $1/T$ (K) and reaction rate constant k_s follow $k_s = 48873e^{-4.88/RT}$ with activation energy = 4.88 kJ. The relationship between time t and r_c (radius of particles at time t) at various temperatures and the relation between temperature and r_c at various times follows the exponential line equation. If both temperature and time parameters are combined the relation between time and temperature T with r_c will be found as the following equation $\ln r_c = -0.9536 (9E-04T + 0.005t) + 4.9976$.

ACKNOWLEDGMENT

On this occasion the authors would like to thank PT TIMAH who has given REOH and this research at the cost of DIPA in year 2017. Thanks also to Mrs. Suprihati who has helped us out in this research

REFERENCES

- [1]. L. Hu and M. Chen, "Preparation of ultrafine powder: The frontiers of chemical engineering," *J. Mater Chem Phys.*, vol. 43(3), pp. 212–219, 1996.
- [2]. X M. Wu, L. Wang, Z.C. Tan, G.H. Li, S.S. Qu, "Preparation characterization and low-temperature heat capacities of nanocrystalline TiO₂ ultrafine powder," *J. Solid State Chem.*, vol. 156(1), pp. 220–224, 2001.
- [3]. D.S. Yan, "Synthesis and fabrication of nanostructured materials," *J. Inorg Mater.*, vol. 10(1), pp. 1–6, 1995.
- [4]. V.A. Murugan, S. C.Navale, V.Ravi, "Synthesis of nanocrystalline La₂O₃ powder at 100 °C," *J. Mater Lett.*, vol. 60(6), pp. 848–849, 2006.
- [5]. B A A. Balboul, Ei-Roudi A M. Samir E. Othman A G. "Non-Isothermal Studies of The Decomposition Course Of Lanthanum Oxalate Decahydrate," *J. Thermochim Acta.*, vol. 387(2), pp. 109–114, 2002.
- [6]. Petryk J. Kolakowska E. "Cobalt oxide catalysts for ammonia oxidation activated with cerium and lanthanum," *J. Appl. Catal B.*, vol. 24(2), pp. 121–128, 2000.
- [7]. Schweizer T. Samson B N. Hector J R. Brocklesby W S. Hewak D W. Payne D N. "Infrared emission from holmium doped gallium lanthanum sulphide glass," *J. Infrared Phys. Techn.*, vol. 40, pp. 329–335, 1999.
- [8]. Escudero M J. Novoa X R. Rodrigo T. Daza L. "Influence of lanthanum oxide as quality promoter on cathodes for MCFC," *J. Power Sources*, vol. 106(1–2), pp. 196–205, 2002.
- [9]. Chen Zhan-heng. "Rare earth new materials and their application in the field of high technology," *J. Chinese Rare Earths*, vol. 21(1), pp. 53–57, 2001. (in Chinese)
- [10]. Zhang Ke-li. Chen Xiong-bin. XI Mei-yun. Song Li. Zhang Xiao-feng. SUN Ju-tang. Thermal decomposition of lanthanum oxalate decahydrate," *J. Wuhan Univ.*, vol. 42(2), pp. 163–166, 1996. (in Chinese)
- [11]. Yang Q. Tang K B. Wang C R. Qian Y. Zhang S. "PVA-Assisted synthesis and characterization of CdSe and CdTe nanowires," *J. Phys Chem B.*, vol. 106(38), pp. 9227–9230, 2002.
- [12]. Bakiz B., Guinnetion F., Arab M., Benlhachemi A., Gavarria J R. "Elaboration characterization of LaOHCO₃. La₂O₂CO₃ and La₂O₃ phases and their gas solid interactions with CH₄ and CO gases," *J. Condensed Matter*, vol. 12(1), pp. 60–67, 2002.
- [13]. Tang J L., Pan T J., Chen M. "Synthesis of CdS nanoplates using poly (acrylic acid) as precursor by hydrothermal method," *J. Acta Chem Sinica*. vol. 68(4), pp. 325–328, 2010.
- [14]. Zhang H., Yang D R., Li S Z., Ji Y J., Ma X Y., Que D L. "Hydrothermal synthesis of flower-like Bi₂S₃ with nanorods in the diameter region of 30 nm," *J. Nanotechnology*, vol. 15(9), pp. 1122–1125, 2003.
- [15]. Reddy B M., Reddy G K., Khan A., Ganesh I. "Synthesis of monophasic Ce_{0.5}Zr_{0.5}O₂ solid solution by microwave-induced combustion method," *J. Mater Sci.*, vol. 42(10), pp. 3557–3563, 2007.
- [16]. CHI Ru-an. XU Zhi-gao. WU Yuan-xin. WANG Cun-wen. "Optimal conditions for preparing ultra-fine CeO₂ powders in a submerged circulative impinging stream reactor," *J. Rare Earth*, vol. 25(4), pp. 422–427, 2007.
- [17]. Amirpiran Amiria, Gordon, D. Ingram, Nicoleta E. Maynard, IztokLivkb and Andrey V. Bekker. "An Unreacted Shrinking Core Model for Calcination and Similar Solid-to-Gas Reactions," *Chemical Engineering Communications*, vol. 202. Issue 9, 2015.

- [18]. Zhan Guang, YU Jun-xia, XU Zhi-gao, ZHOU Fang, CHI Ru-an. "Kinetics of thermal decomposition of lanthanum oxalate hydrate," *Transactions of Nonferrous Metals Society of China*, vol. 22, pp. 925–934, 2012.
- [19]. J.-C. Grivel, Y. Zhao, M.J. Suarez Guevara, A. Watenphul. "Studies on the thermal decomposition of lanthanum (III) valerate and lanthanum (III) cuprate in argon," *Thermochimica Acta.*, vol. 612, pp. 1–9, 2015.
- [20]. Xiang-hui ZHANG, Chuan HE, Ling WANG, Jing LIU, Miao DENG. "Non-isothermal kinetic analysis of thermal dehydration of $\text{La}_2(\text{CO}_3)_3 \cdot 4\text{H}_2\text{O}$ in air," *Transactions of Nonferrous Metals Society of China*, vol. 24(10). pp. 3378-3385, 2014.
- [21]. Amirpiran Amiria, Gordon D. Ingram, Andrey V., Bekker, IztokLivk, Nicoleta E., Maynard. "A multi-stage.multi-reaction shrinking core model for self-inhibiting gas–solid reactions," *Advanced Powder Technology*, vol. 24(4) , pp. 728–736, 2013.
- [22]. Levenspiel O. *Chemical Reaction Engineering*. Dept of Chem. Engineering. Oregon State University. Wiley Eastern Ltd. New Delhi. Bangalore. Bombay. Calcutta. (1972).
- [23]. Tang W J. Liu Y W. Yang X. Wang C X. "Kinetic studies of the calcination of ammonium metavanadate by thermal methods," *J. Ind Eng Chem Res.*, vol. 43(9), pp. 2054–2059, 2004.
- [24]. Yüksel Altaş, Hüseyin Tel. "Structural and thermal investigations on cerium oxalate and derived oxide powders for the preparation of $(\text{ThCe})\text{O}_2$ pellets," *Journal of Nuclear Materials*, vol. 298(3), pp. 316–320, 2001.
- [25]. Guo-Qiang Zhang, Tian-Yu Guo, Zhong LI. "Effect of calcination temperature on catalytic performance of CuCe/AC catalysts for oxidative carbonylation of methanol," *Journal of Fuel Chemistry and Technology*, vol. 44(6), pp. 674-679, 2016.



Copyright © 2019 Jusami | Indonesian Journal of Materials Science. This article is an open access article distributed under the terms and conditions of the [Creative Commons Attribution-NonCommercial-ShareAlike 4.0 International License \(CC BY-NC-SA 4.0\)](https://creativecommons.org/licenses/by-nc-sa/4.0/).